TOMSK POLYTECHNIC UNIVERSITY

Available online at www.sciencedirect.com

ScienceDirect

Resource-Efficient Technologies 2 (2016) S53–S62

www.elsevier.com/locate/reffit

Research paper

Modeling the adsorption of benzeneacetic acid on CaO_2 nanoparticles using artificial neural network

Sapana S. Madan [a], Kailas L. Wasewar [a,*], S.L. Pandharipande [b]

[a] *Advanced Separation and Analytical Laboratory, Department of Chemical Engineering, Visvesvaraya National Institute of Technology (VNIT), Nagpur, Maharashtra 440010, India*

[b] *Department of Chemical Engineering, LIT, RTMNU, Nagpur, Maharashtra 440010, India*

Received 17 June 2016; received in revised form 6 October 2016; accepted 10 October 2016

Available online 9 November 2016

Abstract

The present work reported a method for removal of benzeneacetic acid from water solution using CaO_2 nanoparticle as adsorbent and modeling the adsorption process using artificial neural network (ANN). CaO_2 nanoparticles were synthesized by a chemical precipitation technique. The characterization and confirmation of nanoparticles have been done by using different techniques such as X-ray powder diffraction (XRD), high resolution field emission scanning electron microscope (HR-FESEM),transmittance electron microscopy (TEM) and high-resolution TEM (HRTEM) analysis. ANN model was developed by using elite-ANN software. The network was trained using experimental data at optimum temperature and time with different CaO_2 nanoparticle dosage (0.002–0.05 g) and initial benzeneacetic acid concentration (0.03–0.099 mol/L). Root mean square error (RMS) of 3.432, average percentage error (APE) of 5.813 and coefficient of determination (R^2) of 0.989 were found for prediction and modeling of benzeneacetic acid removal. The trained artificial neural network is employed to predict the output of the given set of input parameters. The single-stage batch adsorber design of the adsorption of benzeneacetic acid onto CaO_2 nanoparticles has been studied with well fitted Langmuir isotherm equation which is homogeneous and has monolayer sorption capacity.

Keywords: Feed forward neural network; Single-stage batch; Benzeneacetic acid; CaO_2 nanoparticles; Adsorption

1. Introduction

Carboxylic acids have a wide range of application especially in pharmaceuticals, food, and polymers industries. Hence, recovery of carboxylic acids from aqueous solution is an important process in chemical engineering [1]. A number of separation processes have been developed to recover carboxylic acids from aqueous acid [2–5]. Adsorption is low cost and allows an easy operation for the recovery of carboxylic acids [6].

Benzeneacetic acid has a white scale-like crystal look and a honey-like odor at low concentration [7]. It is largely employed in the pharmaceutical industry for making of antibiotics. It is used as a precursor (reactants) in the production of penicillin G [8]. It is an important chemical for the chemical industry. It is found in neroli, rose oil and in many fruits [9]. It has a wide range of biological activity, antibacterial, analgesic, and virucidal properties [10]. It is produced by both fermentation of soya beans using *Bacillus licheniformis* [11,12] and strains of *Bacteroides asaccharolyticus* and *Bacteroides melaninogenicus* subspecies isolated from human and animal sources [13]. It powerfully inhibits the activity of penicillin acylase. Removal of a benzeneacetic from fermentation broth, reaction mixture and waste water is the vital step of complete production process because it directly affects the overall economy of the process [14]. The removal of benzeneacetic acid is required to get higher productivity. Because of these multiple applications in various chemical industries and also medicinal, so it is necessary to remove benzeneacetic acid from aqueous solution is necessary.

CaO_2 nanoparticles are used as an adsorbent for the recovery of benzeneacetic acids because they provide large surface area and are low cost [8]. The basis of separation of benzeneacetic acids (adsorbate) from the feed mixture onto the CaO_2 nanoparticles (solid adsorbent) is governed by the variation

* Corresponding author. Advanced Separation and Analytical Laboratory, Department of Chemical Engineering, Visvesvaraya National Institute of Technology (VNIT), Nagpur, Maharashtra 440010, India. Tel.: +91 712 2801561; fax: +91 712 2801565.

E-mail addresses: k_wasewar@rediffmail.com, klwasewar@chem.vnit.ac.in (K.L. Wasewar).

http://dx.doi.org/10.1016/j.reffit.2016.10.004

Table 1
Summary of ANN applications in adsorption processes.

No.	Adsorbent	Objective of the work	References
1	Hybrid material (Ce-HAHCl)	To study the removal of As (III) from aqueous solution using hybrid material as an adsorbent and ANN was used for modeling of experimental (actual) result	[21]
2	Waste Acorns of Quercus Ithaburensis (WAQI)	To study the adsorption of radioactive Gallium-67 which is employed in nuclear medicine and ANN modeling was used to estimate the adsorption amount	[22]
3	Activated carbon wood charcoal rice husk ash	To predict the removal of efficiency of adsorption of carbonaceous adsorbents to remove phenol and resorcinol from aqueous environment	[23]
4	Shelled *Moringa oleifera* seed (SMOS)	To study the removal of Ni(II) ions from water using SMOS powder by a single layer ANN model	[24]
5	Antep pistachio shells	To study the removal of Pb(II) from aqueous solution by Antep pistachio shells based on 66 experimental sets; three layer artificial neural network model was performed to predict the removal efficiency of Pb(II) ions	[25]
6	Sunflower shells	To study the adsorption potential of shells of sunflower to remove Cu^{2+} ions from aqueous solution using a fixed bed adsorption column	[26]
7	Pumice	To study the use of industrial leachate as adsorbent for the removal of Cu (II)	[27]
8	Magnetic zeolite modified with 2-(3,4dihydroxyphenyl)-1,3-dithiane	To predict the removal of cadmium (II) and copper (II) from water and soil by using synthesized magnetic adsorbent; three layer artificial neural network model was used to estimate the parameters	[28]
9	Hyacinth root	To study the removal of Pb(II) ions from aqueous streams by water hyacinth root; ANN model was employed for the prediction of Pb(II) ions removal	[29]

among the concentrations of the benzeneacetic acids in liquid and solid phases as compared to their equilibrium concentrations. The mathematical models have been used to correlate these equilibrium conditions. Models have failed to predict because of the complexity of the adsorption process [15].

In present work, the experimental data are modeled by using artificial neural networks to resolve the predicted data. Artificial Neural Network (ANN) is a promising alternative modeling tool for various operations involving nonlinear multivariable relationships. It consists of an input and an output layer and one or more hidden layers while input and hidden layers have neuron which receives input values [16]. ANNs act as a black box model which is composed of highly interconnected processing elements called artificial neurons or nodes to solve a specific problem [17,18]. The outcomes were obtained from the ANN software and they are compared with the experimental data to confirm which approach provides superior levels of accuracy [19,20]. Table 1 gives the application of ANN for the removal of benzeneacetic acid in adsorption processes.

Multi Layer Perception (MLP) is a feed forward neural network and is applied in modeling of many chemical engineering applications. It incorporates a network comprising three layers: one input, one output and in between the one hidden layer. The nodes between the two consecutive layers are interconnected by means of weights to find out the layer of neuron. The input layer receives data from the experimental source and are transferred to output layer during hidden layers in the form of array of matrix. The output signal is compared with the target value to produce error signal. Training of the network is carried out to reduce the error by adjusting the weights using suitable algorithm [17,18]. A schematic of the typical structure of an MLP network developed for the adsorption of benzeneacetic acid from aqueous solution using CaO_2 nanoparticles as an adsorbent with two hidden layers containing five neurons each is shown in Fig. 1.

In this work, different network and training algorithms were tried to predict removal of benzeneacetic acid by using CaO_2 nanoparticles, and commented on their performance based on

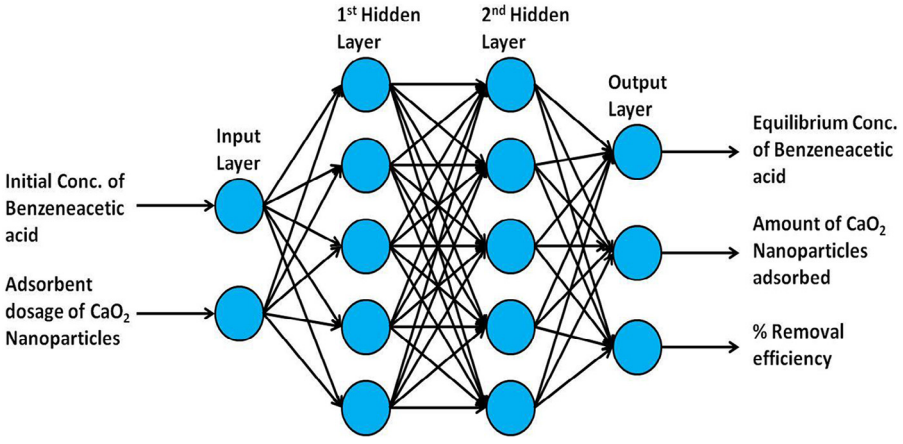

Fig. 1. Neural Network Architecture for ANN model.

determination of coefficient (R^2) and root mean square error (RMSE). The influential parameters, the amount of CaO_2 nanoparticles adsorbent and initial concentration of benzeneacetic acid were investigated. The adsorption isotherms of the prepared adsorbent were studied. An artificial neural network model was developed to predict the behavior of the removal of benzeneacetic acid in the proposed process under various conditions.

2. Experimental section

2.1. Material and methods

Benzeneacetic acid was purchased from Acros Organics (New Jersey, USA). Standard stock solution of benzeneacetic acid of 13.47 g in 1000 mL (0.099 mol/L) was prepared. All solutions were prepared in double distilled water. A digital pH meter (Spectral Lab Instrumental Pvt. Ltd, India) was used to measure pH which was calibrated with three buffers (pH 4.0, 7.0, and 10.0) every day.

2.2. CaO_2 nanoparticles preparation

The detailed CaO_2 nanoparticle synthesis procedure is given in our earlier article [8]. Analytical grade chemicals were purchased and used for the study obtained from Merck (Merck India). Three grams of calcium chloride ($CaCl_2$) were initially added to 30 mL double distilled water followed by addition of 15 mL ammonia solution ($NH_3{\cdot}H_2O$) and then 120 mL of polyethylene glycol (PEG 200). Under constant stirring, 15 mL of 30% hydrogen peroxide (H_2O_2) was added by rate of three drops per minute. Afterward, the solution was stirred for 2 hr and turns yellowish in color. Then, NaOH solution was added until the pH of the solution comes to 11.5. The nanoparticles suspension becomes white in color and was centrifuged at 10,000 rpm for 5 min to separate nanoparticles. The nanoparticles were washed three times by 0.1 N NaOH solutions and two times by distilled water. The final pH of 8.4 for the residue water was obtained. The resultant nanoparticles were dried at 80°C for 2 hours in a vacuum oven.

2.3. Characterization of CaO_2 nanoparticles

X-ray Diffractometer (XRD) analysis [PANalytical X'pert Pro] was performed in 2θ range from 10° to 100° with a step size of 0.01° using Cu target X-ray tube (λ = 1.5406 Å). Morphologies of samples were observed with a high resolution field emission scanning electron microscope (HR-FESEM) from Zeiss, model name ULTRA Plus. It comes with a GeminiÒ column that proposes a theoretical resolution of 1.0 nm at 15 kV. The particle size was confirmed using transmission electron microscopy (TEM) [PHILIPS-CM 200] operated at 20–200 kV. High resolution transmission electron microscopy (HR-TEM) of particles was carried out using JEOL JEM-2100.

2.4. Batch experiments

The interactive effects of CaO_2 adsorbent dosage and initial benzeneacetic acid were in the range of 0.002–0.05 g and 0.03–0.099 mol/L respectively. For each experimental run, 10 mL aqueous benzeneacetic acid solution of known concentration was taken in 100 mL Erlenmeyer flask containing a known mass of CaO_2 nanoadsorbent which was kept in water bath controlled shaker, and once the equilibrium is reached the concentration of benzeneacetic acid (final mixture) was determined by NaOH titration using phenolphthalein indicator. The suspension was then centrifuged at 3000 rpm and CaO_2 nanoparticles were collected. The supernatant was filtered using filter (Whatman) and residual CaO_2 nanoparticles were separated. The experimental values of equilibrium concentration (mol/L), amount of nanoparticles adsorb (mol/L) and % removal efficiency were calculated. ANN models were developed to correlate initial concentration of benzeneacetic acid in feed, adsorbent dosage with equilibrium concentration of benzeneacetic acid on solid and liquid phases and the removal efficiency achieved. In this study, elite-ANN© is employed to develop the entire ANN models [30].

The equilibrium adsorption capacity of benzeneacetic acid (q_e) on the CaO_2 nanoadsorbent was calculated as:

$$q_e = \frac{(C_0 - C_e)}{W} \times V \tag{1}$$

where q_e is the equilibrium capacity of α-toluic acid on the adsorbent (g/g), C_0 (g/L) is the initial concentration of α-toluic acid, C_e is the equilibrium concentration of α-toluic acid in solution after adsorption (g/L), V is the volume of solution (L), and W is the mass of CaO_2 nanoparticles in (g).

The benzeneacetic acid removal efficiency was calculated as:

$$\%\ \alpha\text{-toluic acid removal} = \frac{(C_0 - C_e)}{C_0} \times 100 \tag{2}$$

3. Result and discussion

3.1. Characterization study

X-ray diffraction patterns of CaO_2 are shown in Fig. 2. The 002, 110, 112, 103, 202 and 310 plane reflections are evidently

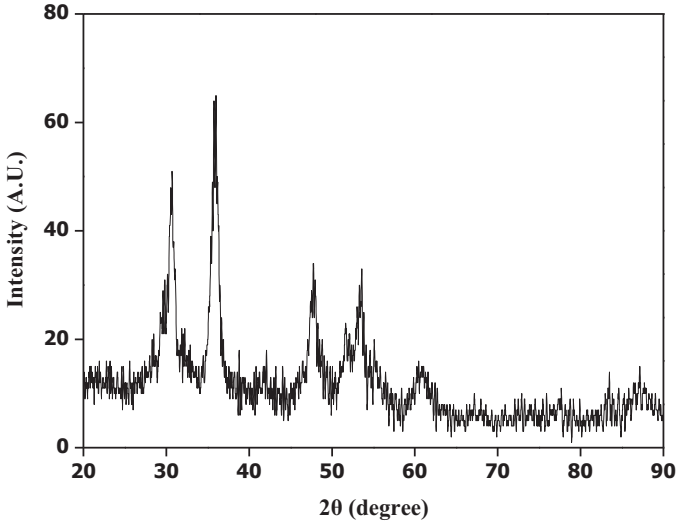

Fig. 2. XRD patterns of CaO_2 nanoparticles.

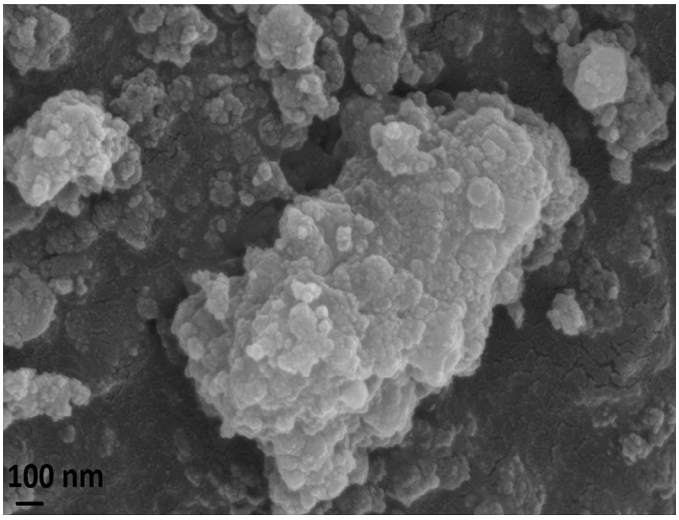

Fig. 3. HR-FESEM images of CaO_2 nanoparticles.

seen and match the reference patterns for CaO_2 (JCPDS) File No. 03-0865 [8]. The average particle size of CaO_2 nanoparticles was determined from the XRD pattern [(112) plane] according to Debye-Scherrer equation:

$$D = K\lambda/(\beta\cos\theta) \quad (3)$$

where K is the Debye-Scherrer constant equal to 0.89, β is the full width at half maximum of (112) peak, θ is the Bragg angle (in radians) and λ is the X-ray wave length equal to 1.5406 Å. The average particle size from Eq. (3) was found to be 16 nm. The morphology of synthesized CaO_2 nanoparticles was studied by the HR-FESEM analysis (Fig. 3). It visibly indicates that CaO_2 nanoparticles showed the aggregated round shape and are generally spherical in shape. Fig. 4(a) and (b) shows TEM and HR-TEM images of CaO_2 nanoparticles with approximately uniform shape and size. The CaO_2 nanoparticles show a very dark image of HR-TEM because CaO_2 nanoparticles possess a higher electron density. The particles were shown as single and isolated because of presence of PEG stabilizer. It can be clearly seen that they are nearly spherical in shape with average particle size of about 10–40 nm.

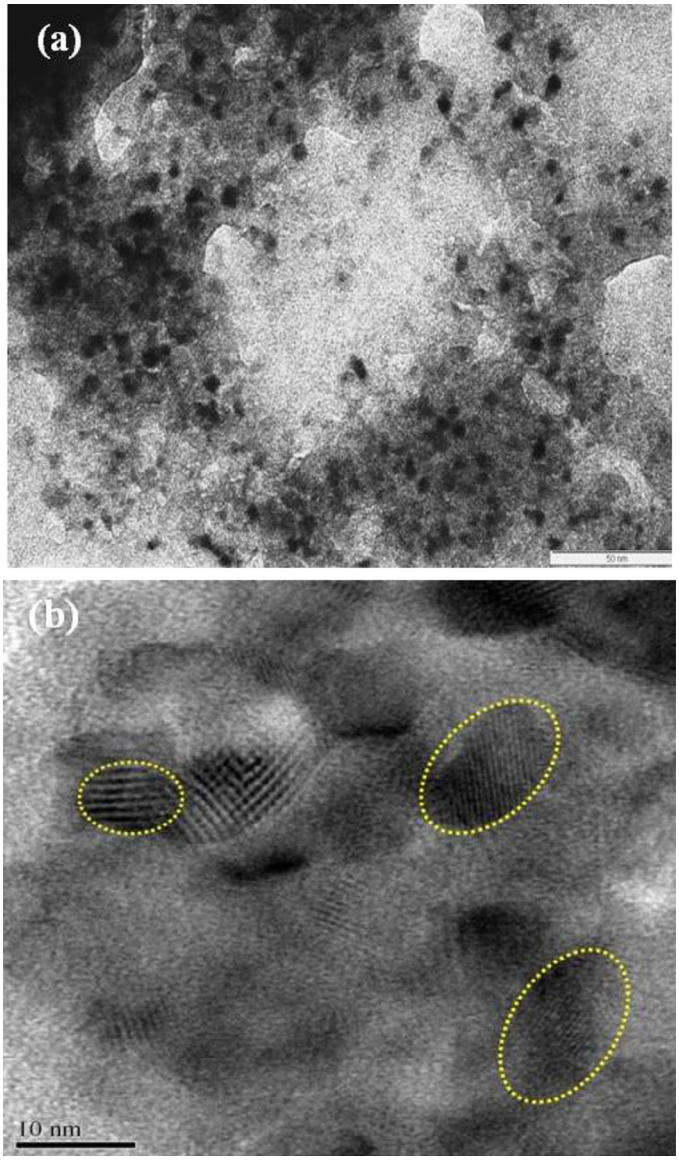

Fig. 4. (a) TEM and (b) HR-TEM images of CaO_2 nanoparticles.

3.2. Influence of adsorbent dosage and initial concentration of benzeneacetic acid

Adsorbent dose and initial concentration are important factors in an adsorption process. The effect of adsorbent dose on the removal of benzeneacetic acid is investigated at a temperature of 22 ± 2°C for 0.002 g–0.05 g keeping all other parameters constant. The removal of benzeneacetic acid increases from 24.75% to 97.47% for initial concentration of 0.099 mol/L with increasing CaO_2 nanoparticles adsorbent dosage. Increase in the adsorbent dosage shows larger surface area and the availability of more adsorption. It is observed that no further increase in the adsorption occurs when CaO_2 nanoparticles dose reaches a value of 0.05 g. The dissimilar equilibrium adsorbent dose is found because increasing the concentration gradient involves higher doses for adsorption. Once the equilibrium dose is achieved, the removal capacity becomes constant and this may be due to collapsing or overlapping of available free sites for adsorption. The effect of initial concentration of benzeneacetic acid varied from 0.04 mol/L to 0.099 mol/L. The removal of benzeneacetic acid increases from 33.3% to 88.3% with a decrease in the concentration of benzeneacetic acid with constant CaO_2 nanoparticles adsorbent dosage of 0.01 g. At low concentration, the number of moles of benzeneacetic acid is small relative to the available adsorption sites on the nanoparticle. Consequently, adsorption becomes independent of initial concentration and as a result adsorption was found to increase. Conversely, at higher concentrations, mainly the adsorption sites will be taken by benzeneacetic acid and the available sites of adsorption become less, hence the removal of efficiency of benzeneacetic acid which depends on the initial decreases in concentration [8,31,32].

Table 2
Total data for ANN modeling of benzeneacetic acid adsorption studies.

Sr. no.	Initial concentration C_o (mol/L)	CaO_2 nanoparticles (g)	Equilibrium concentration C_e (mol/L)	Amount of nanoparticles adsorbed (mol/L)	Removal efficiency (%)
1	0.099	0.002	0.062	0.049	36.87
2	0.099	0.004	0.057	0.056	41.92
3	0.099	0.006	0.063	0.048	35.86
4	0.099	0.008	0.074	0.033	24.75
5	0.099	0.01	0.065	0.046	34.34
6	0.099	0.02	0.045	0.072	54.04
7	0.099	0.03	0.018	0.110	81.82
8	0.099	0.04	0.005	0.127	94.95
9	0.099	0.05	0.002	0.131	97.47
10	0.099	0.01	0.066	0.045	33.30
11	0.08	0.01	0.047	0.046	41.90
12	0.07	0.01	0.040	0.042	43.60
13	0.06	0.01	0.032	0.039	47.50
14	0.05	0.01	0.020	0.041	60.00
15	0.04	0.01	0.006	0.047	86.30
16	0.03	0.01	0.004	0.036	88.30

3.3. ANN models development for adsorption of benzeneacetic acid

The procedure of designing an ANN model is as follows: (i) to specify the number of inputs and outputs for the network, (ii) to create a database of specified input–output variables, (iii) to select the network type, number of layer, number of neurons and activation function of each layer, (iv) training of the ANN network, and (v) to check the performance and accuracy of the trained neural network; altering and retraining of network as per precision level. The training process was carried out until the network output is equivalent with desired output. The weight function reduces the error between the network and desired output. The objective of the work is to correlate two input parameters' initial concentration of benzeneacetic acid and CaO_2 nanoparticles adsorbent dosage with three output parameters that include equilibrium concentration of benzeneacetic acid, CaO_2 nanoparticles adsorbed and % removal efficiency of benzeneacetic acid by developing ANN models. The data set for ANN modeling of benzeneacetic acid adsorption studies as shown in Table 2 is used for this purpose. The features of the ANN topology are shown in Table 3. The ANN model takes around 5000 iterations to converge to final error of 0.0478. The variation of error versus iteration in training mode to develop the model is shown in Fig. 5. The efficacy of ANN model is dependent on its accuracy of prediction. Table 4 and Fig. 6(a–c) show actual (experimental data) and predicted (ANN model's) values of equilibrium concentration, nanoparticles amount after adsorption and % benzeneacetic acid removal efficiencies for training data set. The statistical analysis of the results of the network performance is presented in Table 5. The values of R for the models are closer to 1. The performance of ANN model is calculated by the relative error and mean squared error (MSE). The most important purpose of the process is to determine the weights and to minimize the error. RMSE is calculated by difference between the ANN prediction and the actual response.

$$\mathrm{RMSE} = \left(\frac{1}{n} \sum_{i=1}^{n} (y_i - y_{di})^2 \right)^{1/2} \quad (4)$$

where n is the number of points, y_i is the predicted value and y_{di} is the actual value.

From these graphs, there is a close agreement between the actual and predicted values indicating high accuracy of ANN model developed. However to confirm the claim of accuracy of prediction further, relative error has been calculated and plotted as shown in Fig. 7(a–c) for training data set.

$$\%\ \text{Relative error} = \left(\text{Actual data} - \frac{\text{Predicted data}}{\text{Actual data}} \right) \times 100 \quad (5)$$

The root mean square error (RMSE) of 3.4327, mean percentage error (MPE) of 5.814 and coefficient of determination (R^2) of 0.989 were found for prediction and modeling of benzeneacetic acid removal for the training data set, as shown in

Table 3
Neural network topology.

Number of neurons					RMSE
Input layer	First hidden layer	Second hidden layer	Third hidden layer	Output layer	Training data set
2	00	05	05	3	0.0478

Number of iteration: 5000, time: 25,413 millisecond
Input parameters: initial concentration, amount of CaO_2 nanoparticles (adsorbent)
Output parameters: equilibrium concentration, amount of CaO_2 nanoparticles adsorbed, removal efficiency

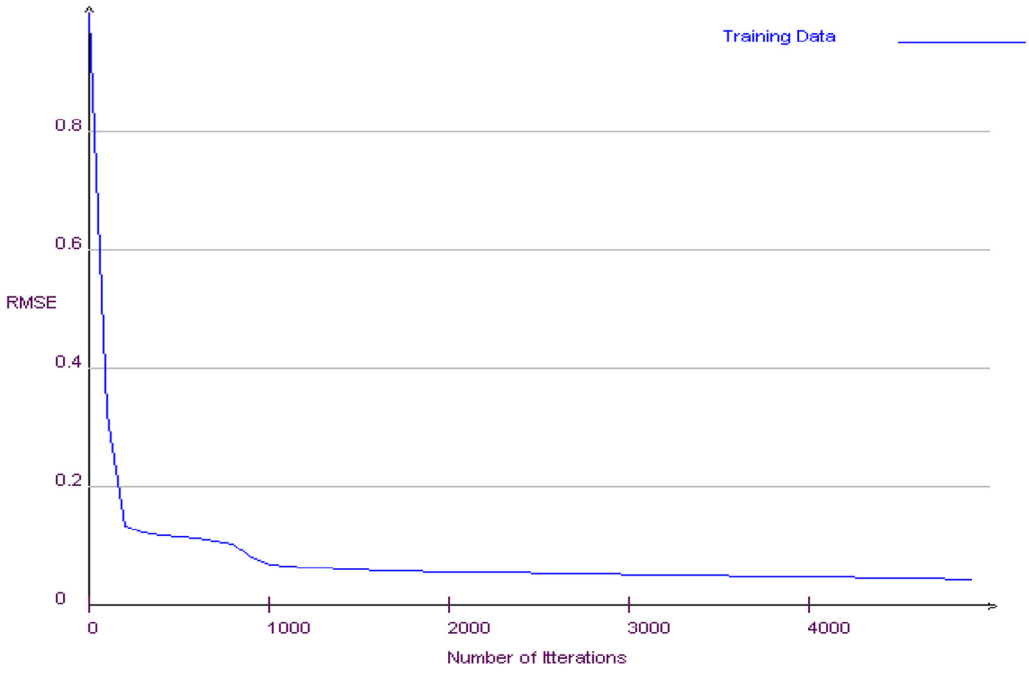

Fig. 5. Performance graph (error versus iteration in training mode).

Table 5. The RMSE, R^2, and APE values are within an acceptable range. The range of correlation coefficients is extremely close to 1, which indicates outstanding agreement between the experimental and the ANN predicted results.

3.4. Adsorption isotherm

The isotherm results were examined using Langmuir and Freundlich isotherms. The function of the adsorption isotherms is to relay the adsorbate concentration in the bulk and the adsorbed amount at the interface [33]. Langmuir isotherm shows monolayer adsorption over the homogeneous CaO_2 nanoparticle adsorbent surface [34,35]. The Freundlich isotherm considers the heterogeneous surface of an adsorbent and is used to describe the adsorption data [36]. Analysis of adsorption isotherms of benzeneacetic acid by CaO_2 nanoparticles is given in Fig. 8. It is important to develop the equation which is used for design purposes.

The linear forms of the Langmuir and the Freundlich equations are:

$$\frac{C_e}{q_e} = \frac{1}{K_L} + \frac{a_L}{K_L} C_e \tag{6}$$

Table 4
Comparison of ANN model output and experimental values input for training data.

Sr. no.	Benzeneacetic acid removal efficiency (%)		Benzeneacetic acid equilibrium concentration (mol/L)		Amount of CaO_2 nanoparticles adsorb (mol/L)	
	Experimental (actual) values	ANN predicted values	Experimental (actual) values	ANN predicted values	Experimental (actual) values	ANN predicted values
1	36.87	34.09	0.063	0.065	0.050	0.045
2	41.92	34.09	0.058	0.065	0.057	0.046
3	35.86	34.2	0.064	0.065	0.048	0.046
4	24.75	34.48	0.075	0.065	0.033	0.046
5	34.34	35.03	0.065	0.064	0.046	0.047
6	54.04	53.26	0.046	0.047	0.073	0.071
7	81.82	81.98	0.018	0.018	0.110	0.111
8	94.95	94.40	0.005	0.006	0.128	0.126
9	97.47	96.42	0.003	0.004	0.131	0.129
10	33.30	35.03	0.066	0.064	0.045	0.047
11	41.90	40.33	0.047	0.048	0.046	0.044
12	43.60	43.27	0.040	0.04	0.042	0.043
13	47.50	47.67	0.032	0.032	0.039	0.041
14	60.00	61.06	0.020	0.019	0.041	0.041
15	86.30	83.89	0.006	0.007	0.047	0.041
16	88.30	90.99	0.004	0.004	0.036	0.041

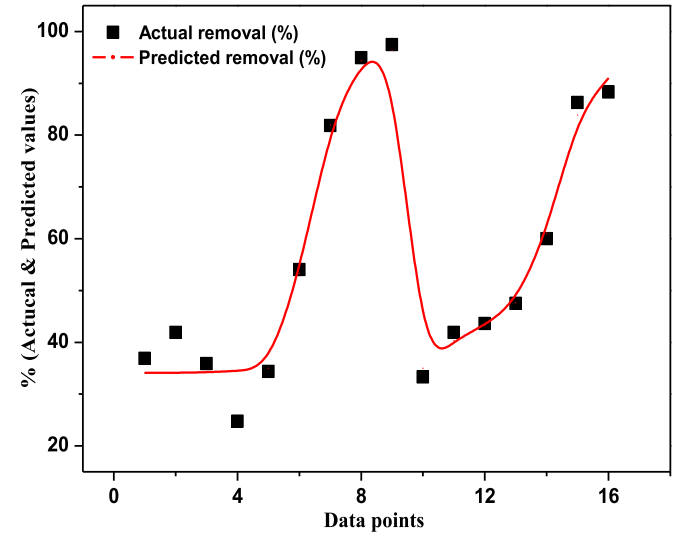

(a)

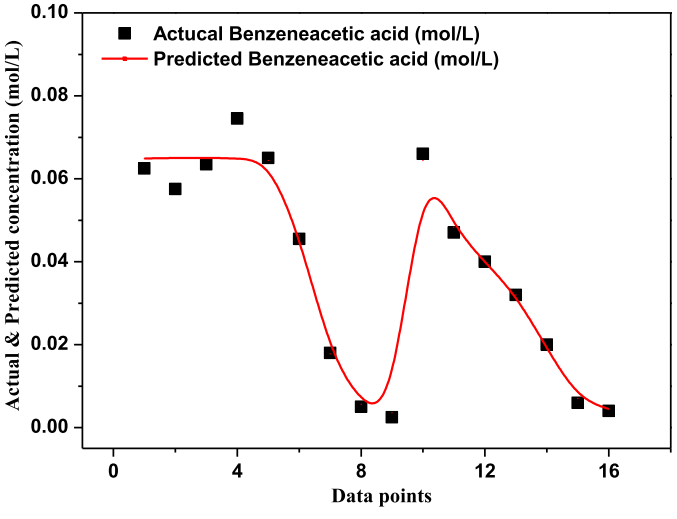

(b)

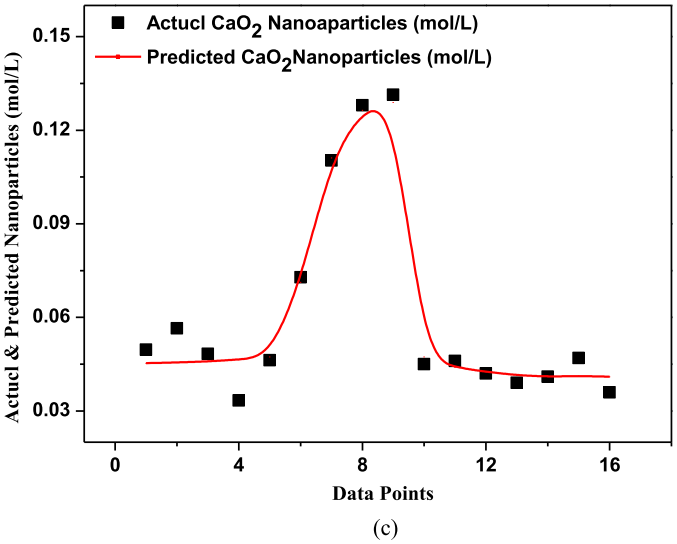

(c)

Fig. 6. Comparison of actual and predicted values of (a) removal efficiency of benzeneacetic acid, (b) equilibrium concentration of benzeneacetic acid, and (c) amount of CaO_2 nanoparticles after adsorption for training data set.

Table 5
Statistics of neural network models.

Models parameters	RMSE	Coefficient of determination	Average percentage error
Benzeneacetic acid removal efficiency (%)	3.432	0.989	5.814
Benzeneacetic acid equilibrium concentration (mol/L)	0.003	0.992	8.365
Amount of CaO_2 nanoparticles adsorbed (mol/L)	0.005	0.987	7.768

$$\log q_e = \log K_F + \frac{1}{n}\log C_e \tag{7}$$

where q_e is the amount of benzeneacetic acid adsorbed per unit mass of CaO_2 nanoparticles adsorbent (g/g), C_e is the equilibrium concentration of benzeneacetic acid in solution (g/L), K_L (L/g) and a_L (L/g) are the Langmuir isotherm constants and K_F (L/g) and n are the Freundlich isotherm constants.

In order to best fit of experimental data against the model predictions, error analysis was performed by using the normalized deviation (ND) and normalized standard deviations (NSD) through Eqs. (8) and (9), respectively [37,38].

$$ND = \frac{100}{n}\sum\left|\frac{q_{e(\exp)} - q_{e(pred)}}{q_{e(\exp)}}\right| \tag{8}$$

$$NSD = 100\sqrt{\frac{\sum\left(q_{e(\exp)} - q_{e(pred)}\right)/q_{e(\exp)}\right)^2}{n}} \tag{9}$$

$q_{e(exp)}$ and $q_{e(pred)}$ are the experimental and predicted adsorption capacity (g·g−1), respectively, and N is the number of observations made.

Langmuir isotherm fits well with the experimental data ($R^2 = 0.99$), whereas the low correlation coefficients $R^2 = 0.71$ show poor agreement of Freundlich isotherms with the experimental data. The values of the constant K_L and a_L are 20.83 L/g and 4.604 L/g respectively. The values of the constant K_F and n values are 2.95 L/g and 4.90 respectively. ND and NSD values for Langmuir isotherm are 4.892 and 10.546 and for Freundlich isotherm are 9.267 and 21.431 respectively. The minimum values of ND and NSD are found for the Langmuir model. Langmuir isotherm offers better correlation with the experimental data as compared to Freundlich isotherm.

3.5. Design of batch adsorption system from isotherm data

Isotherm data can be used to predict the design of batch adsorption system. Mass balance study presents superior information in industrial point of view. It provides better information of the quantity of CaO_2 nanoparticles (adsorbent) required for achieving desired efficiency when treating with benzeneacetic acid [39–41]. A schematic diagram of a single-stage batch adsorber mass balance diagram is shown in Fig. 9. Consider W as the mass of CaO_2 nanoparticles (g), V as the volume of benzeneacetic acid concentration (L), C_0 as the initial concentration of benzeneacetic acid, C_e as the equilibrium

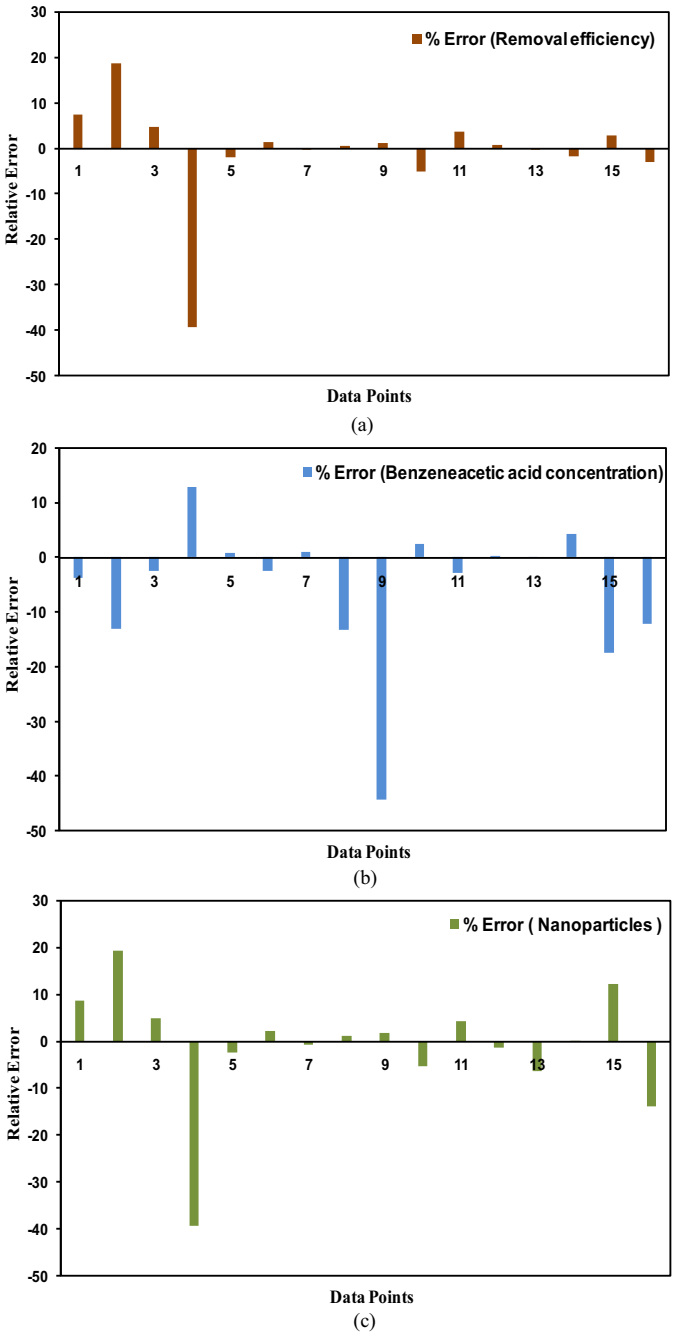

Fig. 7. % Relative error for (a) removal efficiency of benzeneacetic acid, (b) equilibrium concentration of benzeneacetic acid, and (c) amount of CaO_2 nanoparticles adsorbed for training data set.

concentration of benzeneacetic acid, and q_0 and q_1 are g of adsorbed per g of CaO_2 nanoparticles (adsorbent).

The mass balance for the benzeneacetic acid in the single-stage batch adsorption systems is given by:

$$V(C_0 \quad C_1) = W(q_0 q_1) \tag{10}$$

For equilibrium condition,

$$C_1 = C_e,\ q_1 = q_e,\ q_0 = 0 \tag{11}$$

Eq. (10) can be modified and rearrange as:

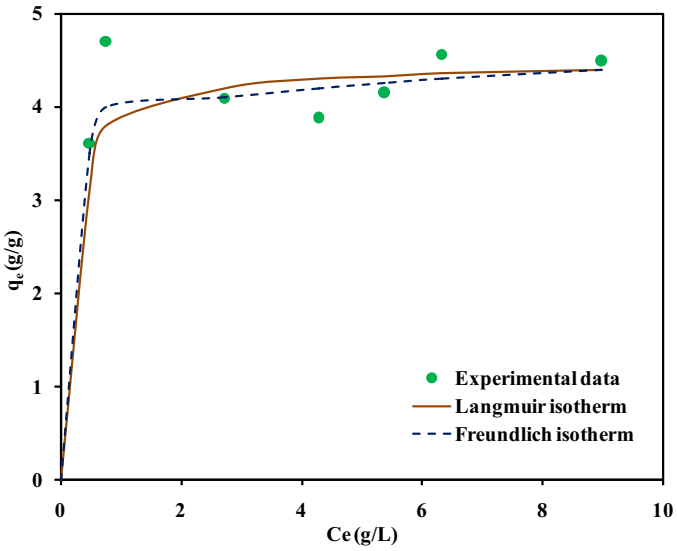

Fig. 8. Adsorption isotherms of benzeneacetic acid by CaO_2 nanoparticles.

$$\frac{W}{V} = \frac{(C_0 - C_e)}{q_e} \tag{12}$$

The Langmuir isotherm is the best fit to experimental data for adsorption of benzeneacetic acid on CaO_2 nanoparticles. Therefore, the Langmuir equation can be best substituted for q_e in Eq. (12)

$$\frac{W}{V} = \frac{C_0 - C_e}{\dfrac{K_L C_e}{1 + a_L C_e}} \tag{13}$$

where $q_e = \dfrac{K_L C_e}{1 + a_L C_e}$.

Fig. 10 shows a plot derived from Eq. (13) for 88.3% removal of benzeneacetic acid at different volumes and required amount of CaO_2 nanoparticles; initial concentration of benzeneacetic acid as 4.08 g/L is assumed. The amount of CaO_2

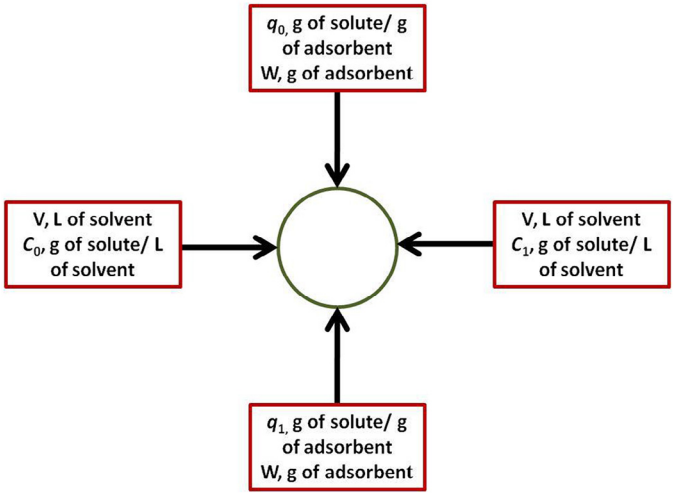

Fig. 9. A single-stage batch adsorber mass balance diagram.

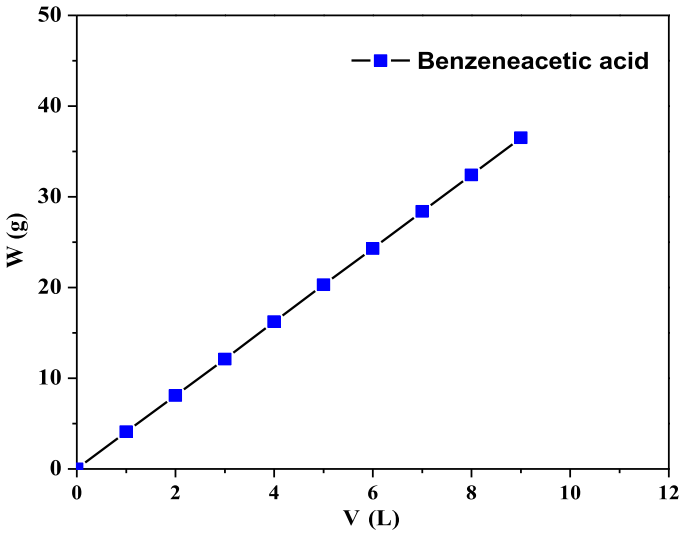

Fig. 10. CaO_2 nanoparticles (adsorbent) mass (W) against volume of benzeneacetic acid (V) treated for 88.3% removal efficiency.

nanoparticles required for the 88.3% removal of benzeneacetic acid solution of concentration 4.08 g/L was 4.1, 8.1, 12.1, 16.2, and 20.3 for volumes of 1, 2, 3, 4, and 5 respectively.

4. Conclusion

CaO_2 nanoparticles have been successfully synthesized by a chemical precipitation method. The synthesized CaO_2 nanoparticles were characterized by various analytical techniques such as XRD, HR-FESEM, TEM, and HR-TEM. The present study clearly revealed that synthesized CaO_2 nanoparticles were excellent alternative for removal of benzeneacetic acid from aqueous solution. An analysis of the correlation between the predicted results of the designed ANN model and the actual (experimental data) was carried out. The results obtained from the ANN model showed that the values of the coefficient of determination (R^2) and root mean square error (RMSE) were found to be 0.989 and 3.432 for benzeneacetic acid removal. The Langmuir is the best model for fitting experimental data and it is used for the design of batch adsorption system. At constant percentage, the mass of CaO_2 nanoparticles as adsorbent is achieved for benzeneacetic acid removal from aqueous solution. The unique feature of the ANN modeling technique is simple to execute, cost-effective, highly accurate and needs less time.

Acknowledgements

We gratefully thank SAIF IIT Bombay for carrying out the TEM facility and SAIF NEHU Shillong for providing the HRTEM facility. We also thank Metallurgical & Materials Engineering Department, VNIT for providing XRD facility.

References

[1] O. Ozcan, I. Inci, Y.S. Asci, Multiwall carbon nanotube for adsorption of acetic acid, J. Chem. Eng. Data 58 (2013) 583–587.
[2] K.L. Wasewar, C.K. Yoo, Intensifying the recovery of carboxylic acids by reactive extraction, in: International Conference on Chemistry and Chemical Engineering, vol. 38, IACSIT Press, Singapore, 2012.
[3] Y.S. Asci, I.M. Hasdemir, Removal of some carboxylic acids from aqueous solutions by hydrogels, J. Chem. Eng. Data 53 (2008) 2351–2355.
[4] K. Schugerl, W. Degener, Recovery of low molecular weight compounds from complex aqueous mixtures by extraction, Int. Chem. Eng. 32 (1992) 29–40.
[5] J. Hartl, R. Marr, Extraction processes for bioproduct separation, Sep. Sci. Technol. 28 (1993) 805–819.
[6] O.N. Arslanoglu, I. Inci, S.S. Bayazit, Purification of biotechnological carboxylic acids with an adsorption method using single-walled carbon nanotubes, J. Chem. Eng. Data 55 (2010) 5663–5668.
[7] K.K. Athankar, K.L. Wasewar, M.N. Varma, D.Z. Shende, H. Uslu, Stoichiometric and spectroscopic study of reactive extraction of phenylacetic acid with tri-*n*-butyl phosphate, Chem. Biochem. Eng. Q. 29 (2015) 385–394.
[8] S.S. Madan, A. Upwanshi W, K.L. Wasewar, Adsorption of α-toluic acid by calcium peroxide nanoparticles, Desalination Water Treat. 57 (2016) 16507–16513.
[9] K.K. Athankar, K.L. Wasewar, M.N. Varma, D.Z. Shende, H. Uslu, Extractive separation of benzylformic acid with phosphoric acid tributyl ester in CCl_4, decanol, kerosene, toluene, and xylene at 298 K, J. Chem. Eng. Data 60 (2015) 1014–1022.
[10] J. Gunjan, D. Awadh, Synthesis and biological evaluation of some phenyl acetic acid hydrazone derivatives, Int. Res. J. Pharm. 2 (2011) 110–112.
[11] S.H. Kim, J.L. Yang, Y.S. Song, Physiological functions of chungkuk-jang, Food Ind. Nutr. 4 (1999) 40–46.
[12] H.K. Yong, H.S. Choi, S.H. Hur, J.H. Hong, Antimicrobial activities of viscous substances from chungkukjang fermented with different Bacillus spp, J. Food Hyg. Saf. 16 (2001) 288–293.
[13] F.S. Kaczmarek, A.L. Coykendall, Production of phenylacetic acid by strains of Bacteroides asaccharolyticus and Bacteroides gingivalis (sp. nov.), J. Clin. Microbiol. 12 (1980) 288–290.
[14] K.K. Athankar, M.N. Varma, D.Z. Shende, C.K. Yoo, K.L. Wasewar, Reactive extraction of phenylacetic acid with tri-n-butyl phosphate in benzene, hexanol, and rice bran oil at 298 K, J. Chem. Eng. Data 58 (2013) 3240–3248.
[15] S.L. Pandharipande, A.R. Deshmukh, Artificial neural network approach for modeling of Ni(II) adsorption from aqueous solution using Aegle marmelos fruit shell adsorbent, Int. J. Eng. Sci. Emerg. Technol. 4 (2013) 27–36.
[16] M. Ghaedi, A.M. Ghaedi, A. Ansari, F. Mohammadi, A. Vafaei, Artificial neural network and particle swarm optimization for removal of methyl orange by gold nanoparticles loaded on activated carbon and tamarisk, Spectrochim. Acta [A.] 132 (2014) 639–654.
[17] J.A. Anderson, An Introduction to Neural Networks, Prentice-Hall of India, Pvt Ltd, New Delhi, 1999.
[18] S.L. Pandharipande, An Introduction to Artificial Neural Networks, Dennett Publications, Nagpur, 2008.
[19] D. Svozil, V. Kvasnicka, J. Pospichal, Introduction to multi-layer feed-forward neural networks, Chemometr. Intell. Lab. Syst. 39 (1997) 43–62.
[20] J.M. Zurada, Introduction to Artificial Neural Systems, PWS Publishing Company, 1992.
[21] S. Mandal, S.S. Mahapatra, M.K. Sahu, R.K. Patel, Artificial neural network modelling of As(III) removal from water by novel hybrid material, Process Saf. Environ. Prot. 93 (2015) 249–264.
[22] H. Eroglu, M. Aktan, G. Akkaya, Artificial neural network (ANN) modeling and analysis of radioactive Gallium-67 adsorption from aqueous solution with waste acorns of Quercus Ithaburensis, J. Chem. Eng. Data 56 (2011) 1910–1917.
[23] R.M. Aghav, S. Kumar, S.N. Mukherjee, Artificial neural network modeling in competitive adsorption of phenol and resorcinol from water environment using some carbonaceous adsorbents, J. Hazard. Mater. 188 (2011) 67–77.

[24] R.K. Rohit, K. Abhishek, J.K. Arora, M.M. Srivastava, S. Srivastava, Neural network modeling for Ni (II) removal from aqueous system using shelled Moringa oleifera seed powder as an agricultural waste, J. Water Resource Prot. 2 (2010) 331–338.

[25] K. Yetilmezsoy, S. Demirel, Artificial neural network (ANN) approach for modeling of Pb (II) adsorption from aqueous solution by Antep pistachio (Pistacia vera L) shells, J. Hazard. Mater. 153 (2008) 1288–1300.

[26] E. Oguz, M. Ersoy, Removal of Cu^{2+} from aqueous solution by adsorption in a fixed bed column and neural network modeling, Chem. Eng. J. 164 (2010) 56–62.

[27] N.G. Turan, B. Mescib, O. Ozgonenel, The use of artificial neural networks (ANN) for modeling of adsorption of Cu(II) from industrial leachate by pumice, Chem. Eng. J. 171 (2011) 1091–1097.

[28] M. Shirani, A. Akbari, M. Hassani, Adsorption of cadmium (II) and copper (II) from soil and water samples onto a magnetic organozeolite modified with 2-(3,4-dihydroxyphenyl)-1,3-dithiane using an artificial neural network and analysed by flame atomic absorption spectrometry, Anal. Methods 7 (2015) 6012–6020.

[29] T. Mitra, B. Singha, N. Bar, S.K. Das, Removal of Pb (II) ions from aqueous solution using water hyacinth root by fixed-bed column and ANN modeling, J. Hazard. Mater. 273 (2014) 94–103.

[30] S.L. Pandharipande, Y.P. Badhe, Elite-ANN©. ROC No SW-1471/2004. 2004.

[31] M. Ganesapillai, P. Simha, The rationale for alternative fertilization: equilibrium isotherm, kinetics and mass transfer analysis for urea-nitrogen adsorption from cow urine, Resour. Effic. Technol. 1 (2015) 90–97.

[32] V.K. Gupta, B. Gupta, A. Rastogi, S. Agarwal, A. Nayak, A comparative investigation on adsorption performances of mesoporous activated carbon prepared from waste rubber tire and activated carbon for a hazardous azo dye – acid Blue 113, J. Hazard. Mater. 186 (2011) 891–901.

[33] J. Eastoe, J.S. Dalton, Dynamic surface tension and adsorption mechanisms of surfactants at the air water interface, Adv. Colloid Interface Sci. 85 (2000) 103–144.

[34] I. Langmuir, The adsorption of gases on plane surfaces of glass, mica and platinum, J. Am. Chem. Soc. 40 (1918) 1361–1403.

[35] S.S. Madan, K.L. Wasewar, C. Ravi Kumar, Adsorption kinetics, thermodynamics, and equilibrium of a-toluic acid onto calcium peroxide nanoparticles, Adv. Powder Technol. (2016) doi:10.1016/j.apt.2016.07.024.

[36] H.M.F. Freundlich, Over the adsorption in solution, J. Phys. Chem. 57 (1906) 385–471.

[37] M.G. Pillai, P. Simha, A. Gugalia, Recovering urea from human urine by bio-sorption onto microwave activated carbonized coconut shells: equilibrium, kinetics, optimization and field studies, J. Environ. Chem. Eng. 2 (2014) 46–55.

[38] P. Simha, A. Yadav, D. Pinjari, A.B. Pandit, On the behaviour, mechanistic modelling and interaction of biochar and crop fertilizers in aqueous solutions, Resour. Effic. Technol. 2 (2016) 133–142.

[39] M. Ozacar, I.A. Sengil, Equilibrium data and process design for adsorption of disperse dyes onto alunite, Environ. Geol. 45 (2004) 762–768.

[40] G. McKay, M.S. Otterburn, J.A. Aga, Fuller's earth and fired clay as adsorbents for dyestuffs equilibrium and rate studies, Water Air Soil Pollut. 24 (1985) 307–322.

[41] W.J. Thomass, B. Crittenden, Adsorption Technology and Design, Butterwort-Heinemann, Woburn, 1998.